ELSEVIER

Journal of Nuclear Materials 307–311 (2002) 450–454

journal of nuclear materials

www.elsevier.com/locate/jnucmat

# Microstructure evolution in D–T neutron irradiated silver

K. Sugio [a,*], H. Ohkubo [b], I. Mukouda [a], Y. Shimomura [c], C. Kutsukake [d], H. Takeuchi [d]

[a] *Graduate School of Engineering, Hiroshima University, 1-4-1 Kagamiyama, Higashi-Hiroshima 739-8527, Japan*
[b] *Venture Business Laboratory, Hiroshima University, 1-4-1 Kagamiyama, Higashi-Hiroshima 739-8527, Japan*
[c] *Faculty of Engineering, Hiroshima Institute of Technology, 2-1-1 Miyake, Saiki-ku, Hiroshima 731-5193, Japan*
[d] *Department of Fusion Engineering Research, Naka Branch JAERI, Tokai-mura, Ibaraki-ken 319-1195, Japan*

**Abstract**

Irradiation of high purity silver with 14 MeV D–T neutrons was carried out at the fusion neutron source facility in Japan Atomic Energy Research Institute. The range of neutron fluence was $6.1 \times 10^{17}$ to $1.1 \times 10^{21}$ n/m$^2$, which is lower than in earliest D–T neutron irradiations. Thin foil and bulk specimens were irradiated at 288, 423 and 573 K, and observed using transmission electron microscopy. For irradiation at 288 K, the fraction of interstitial clusters in bulk is higher than that in thin foil. In irradiation experiments at 288 and 432 K, the number density of defect clusters is proportional to the neutron fluence to the power of 1.3. In irradiation experiments at 573 K, the defects are mostly stacking fault tetrahedrons (SFTs) and their number density is proportional to the neutron fluence. During isochronal annealing of specimens irradiated at 288 K, disappearance and coalescence of defect clusters were observed, and SFTs were mobile.


## 1. Introduction

14 MeV D–T (fusion) neutron irradiation experiments were performed at RTNS-II in LLNL during 1982–1986. A wide variety of materials were irradiated under a wide range of irradiation conditions, and much knowledge of microstructure evolution of materials irradiated by 14 MeV neutrons was provided [1–11]. This irradiation facility is not in operation at present. In the year 2000, new experiments by fusion neutron irradiation utilizing the fusion neutron source facility (FNS) in Japan Atomic Energy Research Institute (JAERI) [12] were started. Irradiation experiments at various irradiation conditions (temperature and fluence) in fcc metals and bcc metals were systematically carried out. The range of neutron fluence in these experiments covered the lower range of RTNS-II. In this low fluence range, geometrical overlap of cascades begins, and Kiritani et al. [9] proposed that the number of defect clusters increases proportionally to the square of irradiation fluence. In the very low fluence range, it is expected that the cascade structure formed by one collision will be observed. In this paper, we report the results for silver. Thin foil and bulk specimens were irradiated at 288, 423 and 573 K, and were observed using transmission electron microscopy (TEM). In addition, to determine the nature of defect clusters, isochronal annealing experiments were carried out.

## 2. Experimental procedure

The Ag material of nominal 99.9999% purity was purchased from Cominco Inc. Disks of 3 mm diameter and 50 μm thickness were punched out and annealed at about 873 K in a vacuum of $10^{-6}$ Pa. Both thin foil and bulk specimens were prepared. For thin foil specimens, disks were electropolished. Irradiation experiments were carried out at 288, 423 and 573 K. Two types of

* Corresponding author. Tel.: +81-824 24 7857; fax: +81-824 22 7192.
*E-mail address:* ksugio@hiroshima-u.ac.jp (K. Sugio).

0022-3115/02/$ - see front matter 
PII: S0022-3115(02)01208-4

irradiation chambers were designed and assembled for room and high temperature. In the irradiation chamber for 288 K, the specimen temperature was controlled by flowing water. For 423 and 573 K, specimen temperature was controlled using a heater. The vacuum in the chamber was maintained at less than $10^{-5}$ Pa by a turbo molecular pump. Irradiations were performed using the rotating tritium target. D–T fusion neutrons were produced by bombarding a tritium target with deuterons. By placing samples at different distances from the neutron source, neutron flux and fluence were varied. The samples were sandwiched in niobium activation foils to measure the neutron fluence accurately. The range of neutron fluence was $8.0 \times 10^{18}$–$1.5 \times 10^{20}$ n/m$^2$ in present work. Fluences of $10^{18}$ and $10^{20}$ n/m$^2$ are referred to as very low fluence and low fluence, respectively. Bulk specimens were electropolished after radiation cooling. TEM observations were performed with JEOL-2000EX operated at 200 kV. Defect clusters were observed from the [1 1 0] direction with $\mathbf{g} = [0\,0\,2]$ under a $(g, 5g)$ weak beam diffraction condition. The specimen thickness of the foil area under observation was estimated from equal-thickness contour lines.

## 3. Results

### *3.1. Defect structures in D–T neutron irradiated silver at 288, 423 and 573 K*

Fig. 1(a) and (b) show dark field images observed in thin foil specimens irradiated at 288 K. Three kinds of defect images, (1) two parallel lines, (2) triangles and (3) diffuse dots, were seen and examples are indicated by arrows in Fig. 1(a) and (b). Because an image of two parallel lines moved back and forth between two positions under electron illumination, it is an interstitial cluster that relaxes to a bundle of $\langle 1\,1\,0\rangle$ crowdions [13,14]. A triangular image is a stacking fault tetrahedron (SFT), which is observed as a square image when viewed from [0 0 1] direction. The diffuse dot images are interstitial clusters or vacancy clusters, but for the moment are unspecified. (To determine the nature of diffuse dots, we carried out annealing experiments later.) The fraction of crowdion interstitial clusters is very low and under 1%. The fraction of SFT and diffuse dots are 6% and 93%, respectively. Fig. 1(a) and (b) are comparisons of the defect structures between very low fluence ($9.4 \times 10^{18}$ n/m$^2$) and low fluence ($1.2 \times 10^{20}$ n/m$^2$). Defect clusters observed after very low fluence irradiation were isolated, as shown in Fig. 1(a). With increasing fluence, defect groups that contain much more than one defect cluster were observed, as shown in Fig. 1(b).

In thin foil specimen irradiated at 423 K, interstitial clusters of $\langle 1\,1\,0\rangle$ crowdions, SFTs and diffuse dots were observed. Defect clusters were isolated at very low fluence ($8.0 \times 10^{18}$ n/m$^2$) and defect groups were observed at low fluence ($1.5 \times 10^{20}$ n/m$^2$). The defect structure for this temperature is almost identical with that for 288 K. However, the number density of defect clusters is fractionally smaller than that of 288 K, as shown in Fig. 2.

In thin foil specimen irradiated at 573 K, defect clusters are almost all SFTs, and defect groups are not observed at both very low fluence ($9.5 \times 10^{18}$ n/m$^2$) and low fluence ($1.5 \times 10^{20}$ n/m$^2$).

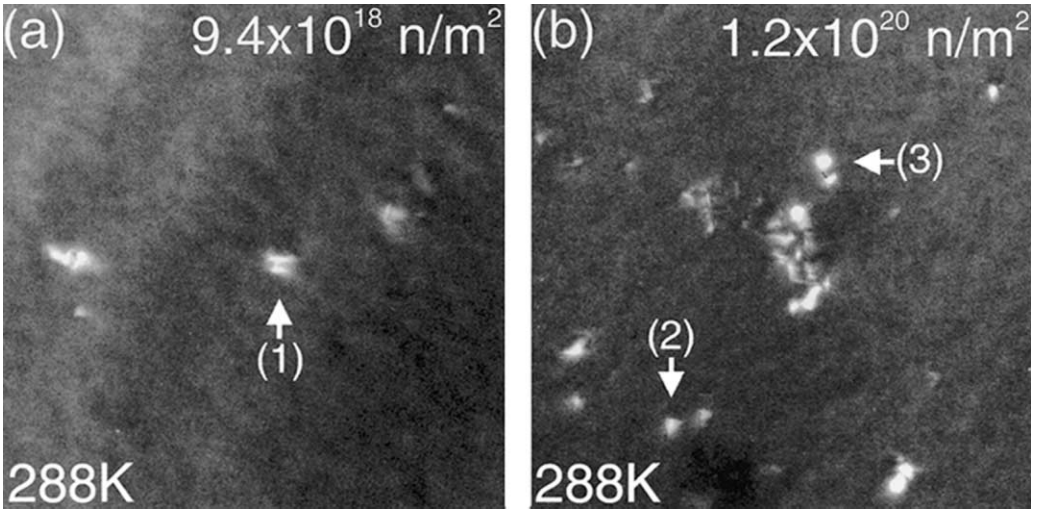


Fig. 1. Defect structures observed in thin foil specimens irradiated at 288 K. Two photographs, very low fluence and low fluence, are shown. Thickness of specimens is (a) 97 nm and (b) 113 nm, respectively.

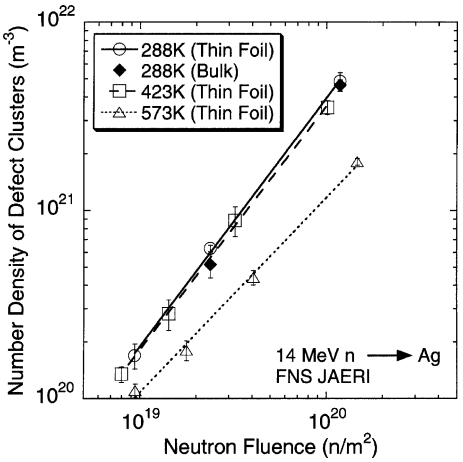


Fig. 2. The relation of number density of defect clusters versus neutron fluence. Solid, dashed and dotted lines are the best fitted to the Eq. (1) for 288, 423 and 573 K, respectively.

### 3.2. The relation of number density of defect clusters versus neutron fluence

Fig. 2 shows number density of defect clusters versus neutron fluence. To estimate number densities, relatively thick parts of specimens (81–113 nm) were chosen and all defect clusters were counted. Plotted values are the average of number densities estimated from three or more photographs. Plotted values are fitted to the equation

$$N_d = A \times (\Phi t)^n \quad (1)$$

for each temperature, where $N_d$ is number density of defect clusters and $\Phi t$ is neutron fluence. Values of the parameters $A$ and $n$ are listed in Table 1. The number density of defect clusters is proportional to the neutron fluence to the power of 1.32 at 288 K. This means that there were invisible defect clusters at very low fluence ($9.4 \times 10^{18}$ n/m$^2$) and some of them became visible with increasing neutron fluence by another cascade collision in close vicinity. Although $n$ for 423 K is lower than that for 288 K, it is thought that identical processes occurred at 288 and 432 K. At 573 K, the number density of defect clusters is proportional to the neutron fluence, and the clusters are almost all SFTs. This means that thermal activation has made defect clusters visible at both very low fluence ($9.5 \times 10^{18}$ n/m$^2$) and low fluence ($1.5 \times 10^{20}$ n/m$^2$).

Table 1
Fitting parameters $A$ and $n$ for each irradiation temperature

| Temperature (K) | $A$ | $n$ |
|---|---|---|
| 288 | $1.5 \times 10^{-5}$ | 1.32 |
| 423 | $4.8 \times 10^{-5}$ | 1.29 |
| 573 | 2.1 | 1.04 |

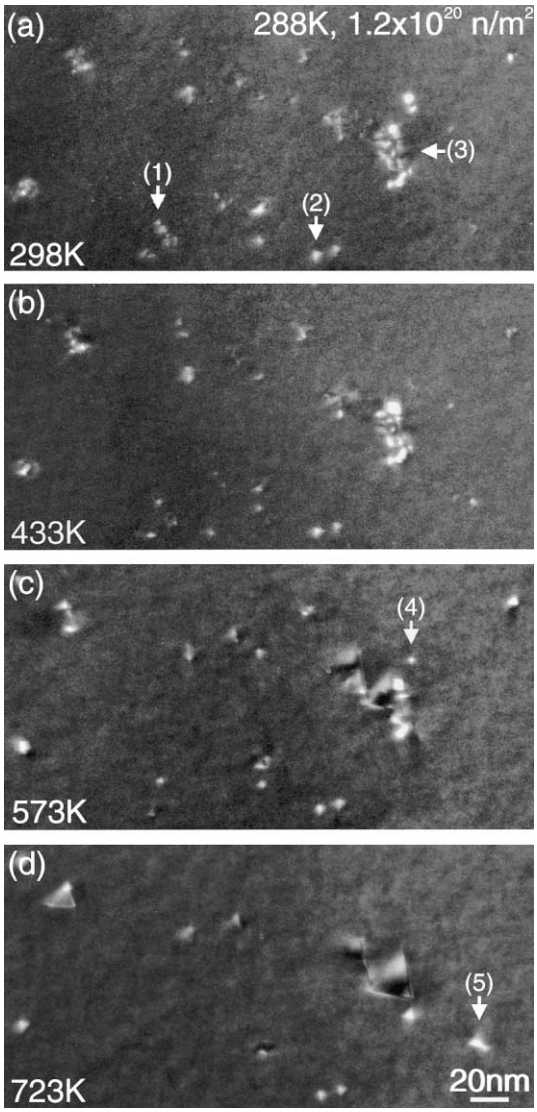


Fig. 3. Changes of defect structures in a thin foil specimen irradiated at 288 K during isochronal annealing. Thickness of specimen is 113 nm. Arrows point out the defect clusters that (1) disappeared, (2) survived, (3) accumulated together, (4) disappeared once and reappeared, and (5) newly appeared.

### 3.3. Isochronal annealing of thin foil and bulk specimens irradiated at 288 K

In order to determine the nature of diffuse dots, isochronal annealing experiments were carried out using the heating stage. Each annealing step was about 10 min. Fig. 3 shows changes of defect structures in a thin foil specimen irradiated at 288 K during isochronal

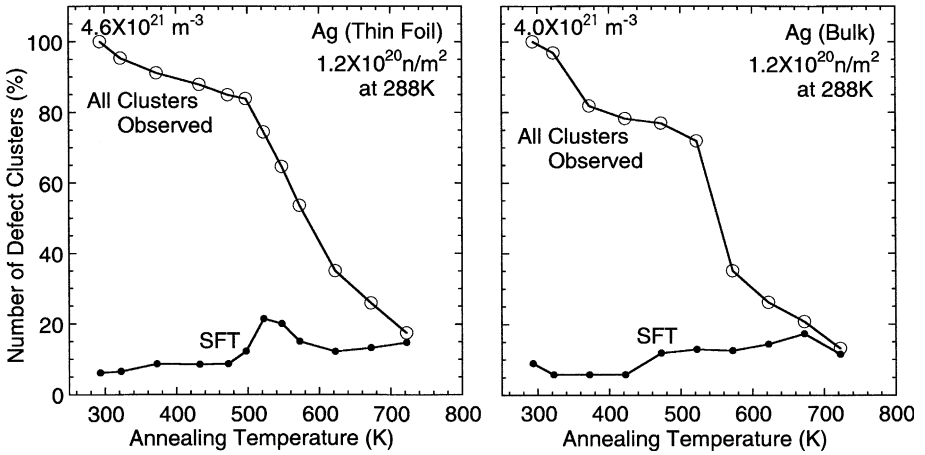


Fig. 4. The variation of number of defect clusters in thin foil and bulk specimens irradiated at 288 K during isochronal annealing.

annealing. From series of these photographs, various behaviors of defect clusters are identified. Arrows in Fig. 3 indicate the defect clusters that (1) disappeared, (2) survived, (3) accumulated together, (4) disappeared once and reappeared, and (5) newly appeared.

Fig. 4 shows the variation of number of defect clusters in thin foil and bulk specimens irradiated at 288 K during isochronal annealing. Differences between thin foil and bulk responses are recognized from these figures. In thin foil, defect clusters decrease gradually at temperatures up to 498 K and the slope becomes large above 498 K. A peak for SFTs is observed at 523 K. In bulk, defect clusters decrease at 373 K instantly and decrease rapidly at 573 K. A peak of SFTs is not observed in bulk. The disappearance of defect clusters can be attributed to four possible processes. The first is the disappearance of interstitial clusters by migration to sink. The second is the disappearance of interstitial clusters by recombination with single vacancies. The third is the disappearance of vacancy clusters by thermal emission of vacancies. The fourth is the disappearance of vacancy clusters by transformation to invisible one. The third and fourth processes are not dominant below 373 K, because probability of thermal emission is low and disappear–reappear defect clusters are rare at this temperature region. Therefore, the first and second processes are thought to be the dominant below 373 K. Assuming that disappeared defects below 373 K are interstitial clusters, the fractions of interstitial clusters in thin foil and bulk is 9% and 18%, respectively. The fraction of interstitial clusters in bulk is higher than that in thin foil.

Table 2
$N_d^{ann}$ and $N_d^{eq}$ are number densities of clusters estimated from annealing and approximated from Eq. (1), respectively

| | Temperature (K) | |
|---|---|---|
| | 423 | 573 |
| $N_d^{ann}$ (n/m$^2$) | $4.0 \times 10^{21}$ | $2.5 \times 10^{21}$ |
| $N_d^{eq}$ (n/m$^2$) | $3.8 \times 10^{21}$ | $1.6 \times 10^{21}$ |
| Difference (%) | 5 | 36 |

## 4. Discussion

Since isochronal annealing experiments and irradiation experiments were carried out at several temperatures, the number density of clusters from annealing experiments can be compared with the number density from irradiation experiments. Neutron fluences of specimens irradiated at 288, 423 and 573 K were slightly different, therefore the clusters number density was approximated by normalizing to a fluence of $1.2 \times 10^{20}$ n/m$^2$ for Eq. (1). Table 2 shows the differences of number density estimated from annealing, $N_d^{ann}$, and approximated from Eq. (1), $N_d^{eq}$. For temperatures of 423 and 573 K, $N_d^{eq}$ values are 5% and 36% lower than $N_d^{ann}$, respectively. This suggests that the defect structure of thin foil specimen annealed at 423 K for 10 min is almost identical with that irradiated at 423 K for 30 h. Consequently, in irradiation experiments at 423 K, it is thought that defect clusters formed by a cascade collision relax to metastable structure within 10 min and are maintained. In contrast, defect structures of thin foil specimen annealed at 573 K for 10 min is different from that irradiated at 573 K for 40 h. This means that relaxation of defect clusters that formed by a cascade collision at 573 K continue more than 10 min and less than 40 h.

Fig. 3 shows that groups of diffuse dots accumulated together and formed large SFT. It seems to be difficult to

explain this accumulation with conventional modeling; vacancies dissolve from vacancy clusters, diffuse by random walk and are absorbed by larger vacancy clusters. In Fig. 3, the amount of vacancies in the groups is not sufficient even if all diffuse dots are assumed to be vacancy clusters. Newly appeared defect clusters are observed in Fig. 3(d), and this suggests the existence of invisible vacancy clusters. From these results, it is thought that vacancy clusters moved as clusters and united to form a large SFT. In addition there is the possibility that invisible vacancy clusters were supplied from surroundings. In Cu [14], it is reported that vacancy clusters move as clusters and SFT coalesce and disappear spontaneously without shrinkage of their size. Moreover computer simulations of molecular dynamics revealed that SFT relax to a movable structure of string-like shape and move as clusters without an evaporation as a single vacancy even at high temperature [15].

## 5. Summary

1. SFT, diffuse dots and a bundle of $\langle 1\,1\,0 \rangle$ crowdions were observed in specimens irradiated at 288 and 423 K. In this temperature region, isolated defect clusters formed during very low fluence irradiation, and they tend to form groups with increasing fluence. The number density of defect clusters formed by irradiation at 288 and 423 K is proportional to the neutron fluence to the power of 1.3. This suggests that there are invisible defect clusters at very low fluence and some of them became visible with increasing neutron fluence by the action of another cascade collision nearby.
2. Defect clusters observed in specimens irradiated at 573 K are almost all SFTs, and defect groups are not observed at both very low fluence and low fluence. The number density of defect clusters formed by irradiation at 573 K is proportional to the neutron fluence. This suggests that invisible defect clusters became visible by thermal activation. At this temperature, disappearance and coalescence of defect clusters occurred, as observed in isochronal annealing experiments. In addition, a series of photographs from isochronal annealing experiments suggests that SFTs are mobile.
3. Isochronal annealing experiments show that more defect clusters disappear below 373 K in bulk than in thin foils. This result suggests that the ratio of interstitial clusters in bulk is higher than in thin foils.

## Acknowledgement

We would like to thank all the staff members of FNS at JAERI for their great help in the D–T fusion neutron irradiation.

## References

[1] M. Kiritani, N. Yoshida, S. Ishino, J. Nucl. Mater. 122–123 (1984) 602.
[2] M. Kiritani, J. Nucl. Mater. 133–134 (1985) 85.
[3] M. Kiritani, Y. Shimomura, N. Yoshida, K. Kitagawa, T. Yoshiie, J. Nucl. Mater. 133–134 (1985) 410.
[4] Y. Shimomura, M. Guinan, M. Kiritani, J. Nucl. Mater. 133–134 (1985) 415.
[5] M. Kiritani, J. Nucl. Mater. 137 (1986) 261.
[6] Y. Shimomura, H. Fukushima, M.W. Guinan, M. Kiritani, J. Nucl. Mater. 141–143 (1986) 816.
[7] Y. Shimomura, H. Fukushima, M. Kami, T. Yoshiie, H. Yoshida, M. Kiritani, J. Nucl. Mater. 141–143 (1986) 846.
[8] T. Yoshiie, S. Kojima, Y. Shimomura, M.W. Guinan, M. Kiritani, J. Nucl. Mater. 141–143 (1986) 860.
[9] M. Kiritani, T. Yoshiie, S. Kojima, Y. Satoh, Radiat. Eff. Def. Solids 113 (1990) 75.
[10] S.J. Zinkle, J. Nucl. Mater. 150 (1987) 140.
[11] A. Horsewell, B.N. Singh, S. Proennecke, W.F. Sommer, H.L. Heinisch, J. Nucl. Mater. 179–181 (1991) 924.
[12] Y. Shimomura, K. Sugio, H. Ohkubo, I. Mukouda, C. Kutsukake, H. Takeuchi, Mater. Res. Soc. Symp. Proc. 650 (2000) R3.8.1.
[13] M. Kiritani, J. Nucl. Mater. 206 (1993) 156.
[14] Y. Shimomura, I. Mukouda, K. Sugio, P. Zhao, Radiat. Eff. Def. Solids 148 (1999) 127.
[15] Y. Shimomura, I. Mukouda, K. Sugio, J. Nucl. Mater. 251 (1997) 61.